JBC Papers in Press. Published on May 11, 2007 as Manuscript M700063200
The latest version is at http://www.jbc.org/cgi/doi/10.1074/jbc.M700063200

CATHESPIN H IS AN FGF10 TARGET INVOLVED IN BMP4 DEGRADATION DURING LUNG BRANCHING MORPHOGENESIS

Jining Lü [1], Jun Qian [1], Daniel Keppler [2, 3], Wellington V. Cardoso [1]
[1]Pulmonary Center, Boston University School of Medicine, Boston, MA 02118, USA;
[2]Department of Cellular Biology & Anatomy and [3]Feist-Weiller Cancer Center, LSUHSC-SHV, School of Medicine, Shreveport, LA 71130

Running title: Cathepsin H during lung branching morphogenesis

Address correspondence to: Wellington V. Cardoso, MD, PhD. Pulmonary Center, Boston University School of Medicine, 715 Albany Street, Boston, MA 02118; Phone: (617) 638-6198; FAX: (617) 536-8093
E-mail: wcardoso@bu.edu

During lung development signaling by fibroblast growth factor 10 (Fgf10) and its receptor Fgfr2b is critical for induction of a gene network that controls proliferation, differentiation and branching of the epithelial tubules. The downstream events triggered by Fgf10-Fgfr2b signaling during this process are still poorly understood. In a global screen for transcriptional targets of Fgf10, we identified Cathepsin H (*Ctsh*), a gene encoding a lysosomal cysteine protease of the papain family, highly upregulated in the developing lung epithelium. Here we show that among other cathepsin genes present in the lung, *Ctsh* is the only family member selectively induced by Fgf10 in the lung epithelium. We provide evidence that, during branching morphogenesis, epithelial expression of Ctsh overlaps temporally and spatially with that of bone morphogenetic protein 4 (Bmp4), another target of Fgf10. Moreover, we show that Ctsh controls the availability of mature Bmp4 protein in the embryonic lung, and that inhibiting Ctsh activity leads to a marked accumulation of Bmp4 protein and disruption of branching morphogenesis. Tightly controlled levels of Bmp4 signaling are critical for patterning of the distal lung epithelium. Our study suggests a potentially novel posttranscriptional mechanism in which Ctsh rapidly removes Bmp4 from forming buds to limit Bmp4 action. The presence of both Ctsh and Bmp4 or Bmp4 signaling activity in other developing structures, such as the kidney, yolk sac and choroid plexus, suggests a possible general role of Ctsh in regulating Bmp4 proteolysis in different morphogenetic events.

Lung organogenesis starts in the mouse at around embryonic day (E) 9.5, when primary buds emerge from the ventro-lateral aspect of the foregut endoderm. At E10.5, secondary buds start to form, and from then on the epithelial tubules undergo a series of patterning events that includes budding, clefting and dichotomous branching to generate the airways and the alveoli. Genetic analysis has implicated a number of signaling molecules, present in the epithelial and mesenchymal layers of growing buds, in controlling cell survival, proliferation, and fate determination during this process. The mechanisms by which expression of these molecules are regulated are complex, and include dynamic induction and spatial restriction of expression, and negative feedback suppression (reviewed in Cardoso and Lu, 2006) (1).

Fibroblast growth factor 10 (Fgf10) is essential for lung formation. No lungs are formed in genetically modified mice in which Fgf10 or its receptor Fgfr2b has been deleted(2-4). Fgf10 is dynamically expressed in the mesenchyme at the presumptive sites of budding. Fgf10 binds to *Fgfr2b* in the epithelium and activates an intra cellular signaling cascade which leads to the migration and proliferation of lung epithelial progenitor cells in emerging buds(2;5). The downstream events triggered by Fgf10-Fgfr2b signaling that are essential for lung branching morphogenesis are still poorly understood. In the process of screening for transcriptional targets of Fgf10, we identified Cathepsin H (*Ctsh*) (EC 3.4.22.16), which encodes a lysosomal cysteine protease of the papain

family, highly upregulated in the developing lung epithelium(6).

Cathepsins represent a heterogeneous group of lysosomal proteases with diverse catalytic mechanisms. Among the eleven members of this family, seven have endopeptidase activity (L, V, S, K, F, B, H), while Cathepsin H exhibits mainly aminopeptidase activity (7). There is accumulating evidence that Cathepsins are critical for tumor invasion and metastasis, and for neovascularization (7-9). The distinct developmental pattern of several cathepsins suggests that these enzymes play specific functions in the embryo (10). Recent information from cathepsin knockout mouse models have largely confirmed this view, and have shown that specific cathepsin deficiencies have far-reaching and discrete consequences on development and homeostasis (11-13). The catalytic events mediated by these enzymes include matrix remodeling by degradation of components of extra cellular matrix(14), intracellular processing of the prohormone thyroglobulin by sequential proteolytic events (15) and modulation of hormone action by turnover of nuclear proteins (16).

Ctsh expression has been previously reported in the lung (17;18). While in the adult lung Ctsh is known to be involved in processing of surfactant proteins B and C(19-21), nothing is known about its potential function in the developing lung. Here we investigate this issue and the biological significance of Ctsh as a target of Fgf10 in the epithelium of developing lung buds. We provide evidence that, during lung branching morphogenesis, epithelial expression of Ctsh overlaps temporally and spatially with that of bone morphogenetic protein 4 (Bmp4), another target of Fgf10. Moreover, we show that Ctsh controls the availability of mature Bmp4 protein in distal lung buds, and that inhibiting Ctsh activity leads to Bmp4 accumulation and disruption of bud formation.

Experimental Procedures

Lung Cultures: Lungs from CD1 mouse embryos were isolated at E11.5-12, placed onto MF-Millipore membrane filters on the top of a metal mesh on tissue culture dish, and cultured for 48-72h with BGjb medium (20 mg/100 ml of ascorbic acid, 1% of inactivated fetal calf serum and 50 units penicillin/streptomycin)(5). In some cultures, heparin beads soaked in either buffer (PBS) or human recombinant FGF10 (100 µg/mL, R&D Systems) were engrafted near distal buds.

For the various experiments, BGJb medium was used with the following reagents: These reagents include: pan-RAR antagonist BMS493 (Bristol Meyers Squibb) or *all-trans* RA (Sigma), Human recombinant Bmp4 or Noggin (a specific inhibitor of Bmp4 signaling/receptor binding, R&D Systems) (22), diazomethane derivatives H-Ser(*O*-Bzl)-CHN_2 (Cathepsin H inhibitor)(23), or Z-Phe-Tyr(*tBu*)-CHN_2 (Cathepsin L inhibitor, BACHEM) or Pepstatin A (Cathepsin D inhibitor) (24), and the general transcription inhibitor actinomycin D (Sigma). Lung cultures were collected either for enzyme activity assay, Western blotting, isolation of total RNA for quantitative real time PCR, immunohistochemistry analysis or *in situ* hybridization, as previously described(25)

For the bud chemoattraction assay, freshly isolated E11.5 distal lung buds were embedded in Matrigel (BD Biosciences, Bedford, MA), and FGF10- or PBS- soaked beads were placed near the distal end of explants shortly before Matrigel solidification(26).Matrigel-embedded explants were then cultured for 72 hours in BGjb medium supplemented with either 1.0 or 2.0 µM Ctsh inhibitor (Ctshi) or DMSO alone.

In situ hybridization: RNA probes were generated using the appropriate RNA polymerases (SP6, T7 or T3) and following the manufacturer's protocol (Ambion). cDNA clones used for probe labeling were obtained from NIA Mouse 15K cDNA Clone Set, distributed by the Microarray Core Facility in Tufts University School of Medicine. The accession numbers for the cDNA clones are: *Ctsh* (BG065250); *Ctsl* (BG065219); *Ctsd* (BG074759) and *Ctsz* (BG064259) (25). *Bmp4* and *Patched* probes (gift from A. McMahon, Harvard University), were labeled as

described(27). Isotopic and non-isotopic (DIG) labeling of RNA probes and whole-mount *in situ* hybridization of freshly isolated or cultured embryonic lungs were performed as previously described(6).

Western blotting and Immunohistochemistry: Western blot analysis was carried out in samples of cultured lungs and yolk sacs, as previously described(25). Primary antibodies were: Anti-mouse Cathepsin H (Polyclonal antibody, Cat#: AF1013, R&D System), Anti-Sprouty2 (rabbit polyclonal antibody, Upstate, Cat# 07-524), anti-α-Tubulin (monoclonal antibody, Sigma, Cat#T9026), anti-Bmp4 (mouse monoclonal antibody, Santa Cruz biotechnology, Cat#sc-12721). Immune-Star ™HRP Chemiluminescent Kit (Bio-Rad) and appropriate secondary antibodies (Bio-Rad) were used for Western blotting detection. Immunohistochemistry was performed in 5 uM paraffin sections using the anti-Ctsh antibody above, and the Cell and Tissue Staining Kits (CTS Series, R&D System) and the PCNA staining kit (Zymed laboratories Inc) according to the manufacture's protocol.

Cathepsin activity assays: Ctsh activity assay was performed as described earlier (28;29). Briefly, embryonic lung cultures were homogenized in a lysis buffer composed of 25-mM MES, adjusted to pH 6. 2, and supplemented with 1-mM EDTA-Na_2, 50-mM NaCl, 1.0% (v/v) Triton X-100, and 250-mM sucrose. Complete lysis of the tissues was achieved by three successive, 5 to 7-sec sonication cycles. Clear supernatants were obtained after centrifugation at 4 ˚C and 10,000 x g for 15 min. The total protein concentration of samples was determined using the microBCA kit from Pierce (Rockford, IL). All enzyme activity measurements were carried out in a calibrated Bio-Tek FLX-800 fluorescence microplate reader, equipped with 355-nm and 460-nm excitation and emission filters, respectively. Samples (3 to 10 µL) were pre-incubated for 20 min at 20 ˚C in Ctsh assay buffer (50 µL final) in the presence of cathepsin inhibitors or DMSO (vehicle control). Aminopeptidase activity of Ctsh was assayed in 25-mM MES, at pH 6.8, containing 50-mM NaCl, 5-mM DTT, 1-mM EDTA-Na_2, 0.05% (v/v) Triton X-100, 50-µM puromycin and 250-mM sucrose using H_2N-Arg-MCA as substrate. Assay buffer (50 µL) containing H_2N-Arg-MCA substrate was added to pre-incubation mixes and fluorescence intensity of the reaction monitored continuously for 30 min at 37 ˚C.

Quantitative real time PCR: Total RNA was isolated from cultured lungs, treated with DNA-free DNase (Ambion), and reversed transcribed (RT) using Superscript II (Invitrogen). cDNA from RT reactions were analyzed by QRT-PCR in an ABI 7000 instrument (Applied Biosystems, Foster City, CA) using primers (*Fgf10*, *Bmp4* and *beta-actin*) obtained from Assays-on-Demand (Applied Biosystems). Reactions were performed in 50 µl using TaqMan PCR universal Master (Applied Biosystem). The relative concentration of RNA for each gene to beta-actin mRNA was determined using the equation $2^{-\Delta C_T}$ where $\Delta C_T = (C_{\text{TmRNA}} - C_{\text{Tbeta actinRNA}})$.

RESULTS AND DISCUSSION

Ctsh is a downstream target of FGF10 in the developing lung epithelium: We have previously characterized the global transcriptional profile of E11.5 mesenchyme-free mouse lung epithelial explants cultured in the presence of recombinant FGF10(6). Along with the morphological changes associated with initial sealing of the epithelium (0h-8h) and bud initiation (8h-24h), we reported a remarkable induction of *Ctsh* mRNA expression (4.5- and 36-fold at 8 and 24 hours, respectively, p=0.02) (Fig. 1A-B).

Although other Cathepsin genes were identified in our array, none were induced by FGF10 like *Ctsh* was (Fig. 1). For example, Cathepsin L (*Ctsl*) showed a statistically significant, but rather modest increase in expression from 0-24h (Fig.1). By contrast, Cathepsin Z (*Ctsz*) expression decreased over time. Cathepsin C (*Ctsc*), Cathepsin D (*Ctsd*) *and* Cathepsin S (*Ctss*) were detected in lung explants, but expression was not significantly

changed in time (Fig.1, and data not shown). Cathepsin B (*Ctsb*) was undetectable under our experimental conditions (data not shown).

To validate the microarray results, first we localized expression of these Cathepsins in the uncultured E11.5-12 lungs by whole mount in situ hybridization (WMISH). While *Ctsh* expression was strong and clearly restricted to distal epithelial buds, *Ctsl, Ctsd*, and *Ctsz* transcripts were present mostly in the mesenchyme with some weak signals in the epithelium (Fig. 2A-D upper panels). Then, we tested inducibility of Cathepsin genes by engrafting heparin beads soaked in recombinant FGF10 or buffer (PBS, control) onto E11.5-12 lung explants, subsequently cultured for 24-48h. WMISH revealed that only *Ctsh* was consistently induced by FGF10 in our assays (Fig 2. A-D bottom panels). High levels of *Ctsh* were found in epithelial cells surrounding the FGF10 bead, but not the PBS bead (Fig.2E-F). Induction of *Ctsh* was restricted to previously reported sites of activation of FGF10-Fgfr2b(2;5). These results were confirmed by isotopic in situ hybridization (ISH) and immunohistochemistry (Fig. 2G, H). Thus, *Ctsh* showed a unique distribution and responsiveness to FGF10 in the developing lung epithelium.

Ctsh expression is spatially and temporally associated with specific developmental events during organogenesis: We speculated that, in the developing lung, Ctsh could function as a critical mediator of Fgf10-induced morphogenesis. A more detailed survey of the Ctsh expression pattern in the developing lung confirmed persistent expression in distal epithelial buds throughout branching morphogenesis in vivo and in vitro (Fig.2A, G, H, J, K). However, surprisingly, no Ctsh expression was detected in the lung epithelium at E9.5-E11, when Fgf10-Fgfr2b signaling is known to be critical for bud induction and growth of the early lung(3;4). Ctsh signals were evident in endothelial cells of the pulmonary artery outside the lung, along the trachea, but not in the lung proper (Fig. 2I, arrow). Epithelial signals were promptly detected in nascent lung buds only after secondary buds formed (E12 onwards, Fig. 2A). Thus, in the developing lung epithelium, induction of primary and secondary buds occurs in the absence of Ctsh. In the E14.5 lung or at equivalent time in culture, Ctsh could be also identified in scattered mesenchymal cells, presumably macrophage precursors, as some of these expressed the macrophage marker F4/80(30) (Fig.2K, blue arrowhead, data not shown). In the adult lung we confirmed Ctsh expression in Type II alveolar epithelial cells, macrophage and endothelial cells (31).

To learn about the overall distribution of Ctsh and to gain insights into its potential role in developmental processes, we performed a comprehensive Ctsh expression analysis in the E7.0-E14.5 mouse embryo. ISH and immunohistochemical (IHC) analysis revealed a highly restricted expression pattern, with strong signals in the visceral endoderm/yolk sac membrane, the epithelium of lung, kidney and choroid plexus, and endothelial cells of a few large blood vessels (Fig.2-3). Together the data suggested that Ctsh may mediate specific events in a limited population of epithelial and mesenchymal-derived cells in the mouse embryo. In the lung epithelium, Ctsh does not seem to function until branching morphogenesis initiates.

RA signaling suppresses FGF10-induced expression of Ctsh in the lung epithelium: The lack of Ctsh expression in the early lung epithelium in spite of the presence of Fgf10-Fgfr2b signaling was intriguing, particularly because Ctsh was highly inducible by FGF10 in our assays. We asked whether an epithelial signal active in the primary lung bud, but not at subsequent stages could be preventing induction of Ctsh by FGF10-Fgfr2b. A recent microarray screen for retinoic acid (RA) targets during organogenesis showed high levels of *Ctsh* expression in vitamin-A deficient rat embryos(32). Furthermore, we have previously shown that RA signaling is highly active in the epithelium of nascent primary buds, but it is subsequently turned off during branching morphogenesis, coincident with the stage when we first observed epithelial expression of Ctsh. We reasoned

that RA might suppress Fgf10-induced Ctsh expression in the lung epithelium. To test this hypothesis, we engrafted FGF10- or PBS-soaked heparin beads onto E11.5 lung explants in which RA signaling was maintained active by treatment with exogenous RA, as previously described (33). Ctsh expression was determined by immunostaining or western blotting and results were compared to lungs cultured under similar conditions in control media, or in media containing a pan-RAR antagonist (BMS493)(34). The antagonist was used here as an additional control to ensure that no RA signaling was activated in the whole explant. Western blotting and immunostaining analysis showed that RA treatment markedly reduced the Ctsh protein levels and prevented FGF10-induced expression of Ctsh in the lung epithelium, effects not seen in control or BMS493-treated cultures (Fig. 4A, B and C; Fig.2H). These results suggest a model in which Fgf10-mediated induction of Ctsh in the lung epithelium occurs only once endogenous RA signaling has been locally turned off. Although due to technical issues we were unable to properly isolate and culture E9.5-10 lungs to test this model, we had additional supporting evidence of RA-Ctsh interaction in a foregut culture system used to study organogenesis *in vitro* (33). Microarray analysis of E8.5 foregut explants cultured for 24h in BMS493 revealed significant upregulation of Ctsh expression compared to controls (fold change: 1.57; p=0.04).Conversely, rescuing RA signaling in retinaldehyde dehydrogenase-2 (*Raldh2*) null foreguts using exogenous RA resulted in marked upregulation of *Ctsh* (fold change: 6.07; p=0.0006)(Chen F., Lu J, and Cardoso W, unpublished observations). Thus, Ctsh may be part of a developmental program that is initially suppressed in primary buds by early signals, such as endogenous RA, but is later on released during branching morphogenesis.

Inhibition of Ctsh activity using H_2N-Ser(O-Bzl)-CHN_2: We investigated the role of Ctsh in the developing lung by inhibiting Ctsh activity selectively in organ culture systems. Pharmacological inhibitors have been widely used for selective blocking of cathepsin function *in vivo* and *in vitro* (9;24;35). Presently, there is only one inhibitor proven to be selective for Ctsh. H_2N-Ser(*O*-Bzl)-CHN_2 (referred onwards as Ctshi) is a strong and irreversible inhibitor of Ctsh, which shows little or no activity towards two other lysosomal cysteine proteases with exopeptidase activity, Ctsb and Ctsc (36). In addition, Ctshi is a diazomethane derivative that penetrates easily across cell membranes, and, thus, is able to block enzyme activity both intracellularly and extracellularly (see below) (37). Since Ctsh has not been studied in organ cultures, first we characterized the effectiveness of Ctsh inhibition in embryonic lung explants. Culturing E11.5-12 lungs with 1.0 or 2.0μM Ctshi for 72 hours led to a 27 % and 69.5% reduction in the total H_2N-Arg-MCA-hydrolyzing activity relative to DMSO vehicle alone (controls), respectively (Fig. 5A, blue bars). Subsequent incubation of these homogenates with an excess of exogenous Ctshi (10 μM) further reduced the total H_2N-Arg-MCA-hydrolyzing activity of the control lungs by 40-50%. In contrast, no further reduction in activity was found in homogenates of Ctshi-treated lungs (compare blue and magenta bars in Fig. 5A). These results indicate that 1.0 or 2.0 μM of Ctshi treatement was sufficient to completely inactivate Ctsh in cultured lungs at 72h. Similar results were obtained by incubating lungs with Ctshi for 12 hours (data not shown), indicating that Ctshi was able to readily diffuse through the lung tissue and effectively inhibit Ctsh activity.

SDS-PAGE and immunoblotting of these lungs showed that Ctshi treatment resulted in qualitative and quantitative changes in size and abundance of mature Ctsh forms, when compared to controls (Fig. 5B). Mature (active) Ctsh typically migrates as two bands: a 28-KD single-chain form and a 22-KD heavy chain of the two-chain form (38;39). A slight increase in molecular weight of the two species in the Ctshi-treated group was consistent with covalent alkylation of the active-site cysteine residue by the diazomethane inhibitor (40). Ctsh protein was more abundant in Ctshi-treated lungs,

presumably due to increased stability, as indicated by the stronger signals in the material isolated from both supernatant and tissue lysates from this group. Inhibition of Ctsh seems to stabilize both the 22 kD and 28 kD species (Fig.5B, upper panel). This suggests that their turnover might require catalytically active Ctsh, either because Ctsh undergoes autocatalytic degradation, or because Ctsh may act on the maturation of another lysosomal protease involved in the turnover of Ctsh. Ctshi treatment of cultured yolk sacs, another tissue expressing high levels of Ctsh, gave results almost identical to those obtained with the cultured lungs (Fig.5 B, bottom).

Ctsh inhibition disrupts lung branching morphogenesis: Analysis of Ctshi-treated lungs showed a significant decrease in the number of distal epithelial buds (26% and 35% reduction relative to control lungs at 1.0- or 2.0-μM Ctshi, respectively) (Fig.6A). Ctshi did not totally prevent, but inhibited lateral epithelial budding and greatly disrupted dichotomous branching. At 2.0 μM Ctshi, epithelial tubules continued to grow and elongate, as indicated by their finger-like appearance and abundant PCNA staining (Fig. 6B). By contrast, treatment of lung explants with selective inhibitors of Ctsl (Z-Phe-Tyr(*tBu*)-CHN_2 at 1.0 or 2.0 μM) or Ctsd (pepstatin A, up to 100 μM), at concentrations previously known to be effective in the lung and other systems (24), resulted in none of the effects described above (Fig. 6C). Thus, neither Ctsd nor Ctsl seems to have a role in lung epithelial branching, which is in agreement with observations reported in Ctsd or Ctsl null mice (41;42).

We asked whether the reduced branching activity observed in Ctshi- treated lungs could be ascribed to an overall decrease in the expression of endogenous Fgf10. This was not the case, as real time PCR assessment of *Fgf10 mRNA* levels in lungs treated with Ctshi, Ctsdi, or Ctsli were essentially similar to DMSO-treated controls (Fig.7A). Moreover, we found that the inhibitory effect of Ctshi in lung bud induction occurred even in the presence of high levels of exogenous FGF10. We cultured in matrigel E11.5 distal lung buds (epithelium and mesenchyme) adjacent to FGF10 or PBS-soaked heparin beads. In this assay, epithelial cells migrate towards the source of FGF10 (beads), leaving mesenchymal cells behind (which do not express Fgfr2b); migration of the embryonic lung epithelium is thus dependent on the FGF10 provided by the beads (26). Applying Ctshi to these cultures resulted in dramatically reduced migration of epithelial cells towards the beads; the overall growth of the explant appeared to be unaffected, as the original gap between the explant and the beads was filled (Fig. 7B-E). Thus, Ctsh activity was likely to play a role in the response of the lung epithelium to Fgf10.

Inhibition of Ctsh selectively stabilizes mature Bmp4 in cultured lungs: We hypothesized that proteolysis by Ctsh could be involved in processing or degradation of a epithelial signal key for branching of the distal lung epithelium. We asked which candidate molecules, also present in E11.5-12 distal epithelial progenitors, could potentially be Ctsh targets. Candidates such as sonic hedgehog (Shh) or Sprouty 2 (Spry2) were less likely to be relevant, as these molecules were already functioning in the lung epithelium since from E9.5-E10, prior to the onset of Ctsh expression. Moreover analysis of Ctshi-treated lungs did not show obvious changes in levels or distribution of *Ptc* transcripts, a readout of Shh pathway activation (data not shown).

We reasoned that Bmp4 could be a prime candidate target of Ctsh in the lung for several reasons. *Bmp4* is expressed in distal lung buds undergoing branching morphogenesis. Neither Bmp4 nor Ctsh is present in the epithelium of primary buds, and their expression in the lung overlaps temporally and spatially from E11-12 onwards (22). Both Bmp4 and Ctsh are induced by Fgf10 in the distal lung epithelium during branching (6;26;27). Furthermore, the migratory activity of the distal epithelium towards an FGF10-soaked bead *in vitro* is also inhibited by exogenous BMP4 (26), an effect that is similar to what we observed when Ctsh

activity is inhibited. Moreover, proper levels of Bmp4 are critical for distal lung development (22;43;44).

We assessed Bmp4 protein levels in control and Ctshi-treated lungs, and we asked whether Ctsh could be involved in degradation of endogenous Bmp4 as the distal lung forms. Interestingly, western blot analysis of Ctshi treated lungs showed that levels of mature Bmp4 (18-KD) were markedly increased after 48 hours (Fig.8B). By contrast, levels of the Bmp4 precursor (51-KD) were comparable to controls (Fig. 8B). This remarkable accumulation of mature Bmp4 protein seemed to occur selectively with Ctshi, since it was not observed by inhibiting the activity of other cathepsins, such as Ctsl or Ctsd, also expressed in the lung (Fig.8C). Moreover, Ctshi stabilized Bmp4, but not other epithelial targets of Fgf10, such as Sprouty2 (Fig. 8C).

The increase in Bmp4 protein could not be ascribed to an increase in *Bmp4* transcription by Ctshi. Quantitative real time PCR showed that Bmp4 mRNA levels were actually slightly decreased in Ctshi treated lungs, compared to control cultures. To prove that Ctshi was exerting its effects in Bmp4 expression via a post-transcriptional mechanism, we cultured control and Ctshi-treated lungs in the presence of actinomycin D (ActD), a known inhibitor of new transcription. Then, we assessed expression of *Bmp4 mRNA* and Bmp4 protein in these samples by real time PCR and Western blot, respectively. As expected, *Bmp4 mRNA* was downregulated by ActD in both conditions, with or without Ctshi (Fig.8D). However, while Bmp4 protein was nearly absent in lungs treated with ActD alone, levels of Bmp4 were greatly increased by treatment with both ActD and Ctshi. These results strongly support the idea that the accumulation of Bmp4 was not due to increased protein synthesis, but rather decreased Bmp4 degradation by Ctshi. As shown in Fig 8.D, ActD had minimal effect in Ctsh expression, and also suggested that toxic effects were not present (Fig. 8D).

We tested whether Ctsh degradation of Bmp4 protein could be demonstrated directly in a test tube. For this we designed an *in vitro* assay using human recombinant mature BMP4 (R&D System) and human CTSH purified from liver (Athens Research Technology). Conservation of these proteins between human and mouse is high (BMP4: 98%; CTSH, 82%). BMP4 (10ng) was incubated with different amounts of CTSH (3500ng, 1750ng, 875ng, 438ng, 219ng, 109ng, 55ng) in a 20ul reaction mixture, at different pHs (50mM of sodium acetate, 3mM of cysteine, 1mM EDTA, pH 6.8 or 5.2), at 37oC for 24 hours (20, 21). Using this approach we could not demonstrate BMP4 cleavage by CTSH (data not shown). Interestingly, by performing western blot analysis of homogenates from E14 lung, liver, kidney, heart, and adult lung we could identify the expected 22KD and 28KD Ctsh bands; the 22KD species, however, was missing in the Ctsh purified from human liver (Supplementary Fig. 2A). The 22KD Ctsh seemed to have been largely lost during the process of purification. We had evidence that this smaller species may be particularly more susceptible to an autocatalytic process in some systems. For example, we found that in homogenates from cultured MLE15 cells (a mouse lung epithelial cell line), the 22KD band is nearly absent. By contrast, inhibiting Ctsh activity in these cells dramatically stabilizes the 22KD species and enhances its signal (Supplementary Fig. 2B).

Although we do not have functional supporting data, we hypothesize that this smaller Ctsh species is the one responsible for Bmp4 cleavage in vivo. This hypothesis could not be tested in vitro using the enzyme we had available because of the lack of 22KD band. This also could not be tested in the MLE15 cells without preventing autocatalytic degradation, as we discussed above. Alternatively, Bmp4 may not be a direct target of Ctsh in the developing lung *in vivo.*

Finally, we asked whether Bmp4 could be involved in the induction of Ctsh in distal lung buds, and found no supporting evidence. Application of either recombinant BMP4 or the Bmp4 antagonist Noggin, alone or in association with FGF10 (in beads) had no effect in Ctsh expression (data not shown). This reinforced the idea of Bmp4 as a downstream target of Ctsh.

CONCLUDING REMARKS

Previous studies have shown that Fgf10-Fgfr2b regulates the transcription of *Bmp4* in developing lung buds. Bmp4 expression correlates with Fgf10-Fgfr2b activity in distal epithelial cells, and its expression is quickly down-regulated in the region between two newly-formed lung buds (26;27). There is accumulated evidence that, in the developing lung, tightly regulated levels of Bmp4 signaling are required for epithelial cell proliferation and differentiation, and to balance the effects of Fgf10 in bud outgrowth and ensure proper bud morphogenesis(44;45). It has been proposed that high levels of Bmp4 in the distal lung epithelium acts as a lateral inhibitor of budding to ensure extension of a single bud, while preventing the appearance of multiple ectopic buds at the tips (26). Here we provide novel evidence that during lung branching morphogenesis, Fgf10 also controls the availability of mature Bmp4 protein in the distal epithelium by locally inducing expression of the cysteine protease Ctsh. Our data suggest that Ctsh may be one of the regulators of Bmp4 availability produced at the tips. Inhibition of Ctsh activity markedly increased Bmp4 expression and resulted in less branched, "finger-like" epithelial structures. The co-localization of both Ctsh and Bmp4 or Bmp4 signaling activity in other developing structures, such as the kidney(46), visceral endoderm, yolk sac (47) and choroid plexus(48) suggests a possible general role for Ctsh in regulating Bmp4 proteolysis in different morphogenetic events.

Bmp4 is synthesized as a propeptide, and is known to be activated by the proprotein convertase (PC) endoprotease Furin through proteolysis at the multibasic -R-S-K-R- motif (49-52). Several studies have implicated Bmp4 activation by Furins in developmental processes in vertebrates. By contrast, the events associated with recycling and degradation of the mature Bmp4 protein in developing structures are less well characterized. We provide evidence that in the distal lung epithelium, the proteolysis mediated by Ctsh does not target the propeptide, but the mature Bmp4. Ctsh is therefore more likely to be involved in degradation or recycling than in maturation of the Bmp4 protein. Tgf beta family ligands are known to undergo receptor-mediated endocytosis and degradation, which may involve Smurf –mediated targeting of these ligands for degradation in the proteasome or lysosome, where presumably Ctsh is present (53-56).

Reference List

1. Cardoso,W.V., and Lu,J. 2006. Regulation of early lung morphogenesis: questions, facts and controversies. *Development* **133**:1611-1624.

2. Bellusci,S., Grindley,J., Emoto,H., Itoh,N., and Hogan,B.L. 1997. Fibroblast growth factor 10 (FGF10) and branching morphogenesis in the embryonic mouse lung. *Development* **124**:4867-4878.

3. Ohuchi,H., Hori,Y., Yamasaki,M., Harada,H., Sekine,K., Kato,S., and Itoh,N. 2000. FGF10 acts as a major ligand for FGF receptor 2 IIIb in mouse multi-organ development. *Biochem. Biophys. Res. Commun.* **277**:643-649.

4. Sekine,K., Ohuchi,H., Fujiwara,M., Yamasaki,M., Yoshizawa,T., Sato,T., Yagishita,N., Matsui,D., Koga,Y., Itoh,N. et al 1999. Fgf10 is essential for limb and lung formation. *Nat. Genet.* **21**:138-141.

5. Park,W.Y., Miranda,B., Lebeche,D., Hashimoto,G., and Cardoso,W.V. 1998. FGF-10 is a chemotactic factor for distal epithelial buds during lung development. *Dev. Biol.* **201**:125-134.

6. Lu,J., Izvolsky,K.I., Qian,J., and Cardoso,W.V. 2005. Identification of FGF10 targets in the embryonic lung epithelium during bud morphogenesis. *J. Biol. Chem.* **280**:4834-4841.

7. Turk,V., Turk,B., and Turk,D. 2001. Lysosomal cysteine proteases: facts and opportunities. *EMBO J.* **20**:4629-4633.

8. Wolters,P.J., and Chapman,H.A. 2000. Importance of lysosomal cysteine proteases in lung disease. *Respir. Res.* **1**:170-177.

9. Urbich,C., Heeschen,C., Aicher,A., Sasaki,K., Bruhl,T., Farhadi,M.R., Vajkoczy,P., Hofmann,W.K., Peters,C., Pennacchio,L.A. et al 2005. Cathepsin L is required for endothelial progenitor cell-induced neovascularization. *Nat. Med.* **11**:206-213.

10. San,S.B., Chan,S.J., and Steiner,D.F. 1986. Differences in cathepsin B mRNA levels in rat tissues suggest specialized functions. *FEBS Lett.* **201**:251-256.

11. Gelb,B.D., Shi,G.P., Chapman,H.A., and Desnick,R.J. 1996. Pycnodysostosis, a lysosomal disease caused by cathepsin K deficiency. *Science* **273**:1236-1238.

12. Toomes,C., James,J., Wood,A.J., Wu,C.L., McCormick,D., Lench,N., Hewitt,C., Moynihan,L., Roberts,E., Woods,C.G. et al 1999. Loss-of-function mutations in the cathepsin C gene result in periodontal disease and palmoplantar keratosis. *Nat. Genet.* **23**:421-424.

13. Reinheckel,T., Deussing,J., Roth,W., and Peters,C. 2001. Towards specific functions of lysosomal cysteine peptidases: phenotypes of mice deficient for cathepsin B or cathepsin L. *Biol. Chem.* **382**:735-741.

14. Chapman,H.A., Riese,R.J., and Shi,G.P. 1997. Emerging roles for cysteine proteases in human biology. *Annu. Rev. Physiol* **59**:63-88.

15. Friedrichs,B., Tepel,C., Reinheckel,T., Deussing,J., von,F.K., Herzog,V., Peters,C., Saftig,P., and Brix,K. 2003. Thyroid functions of mouse cathepsins B, K, and L. *J. Clin. Invest* **111**:1733-1745.

16. Nomura,Y., Nagaya,T., Yamaguchi,S., Katunuma,N., and Seo,H. 1999. Cleavage of RXRalpha by a lysosomal enzyme, cathepsin L-type protease. *Biochem. Biophys. Res. Commun.* **254**:388-394.

17. Buhling,F., Waldburg,N., Kruger,S., Rocken,C., Wiesner,O., Weber,E., and Welte,T. 2002. Expression of cathepsins B, H, K, L, and S during human fetal lung development. *Dev. Dyn.* **225**:14-21.

18. Ishii,Y., Hashizume,Y., Watanabe,T., Waguri,S., Sato,N., Yamamoto,M., Hasegawa,S., Kominami,E., and Uchiyama,Y. 1991. Cysteine proteinases in bronchoalveolar epithelial cells and lavage fluid of rat lung. *J. Histochem. Cytochem.* **39**:461-468.

19. Brasch,F., Ten,B.A., Johnen,G., Ochs,M., Kapp,N., Muller,K.M., Beers,M.F., Fehrenbach,H., Richter,J., Batenburg,J.J. et al 2002. Involvement of cathepsin H in the processing of the hydrophobic surfactant-associated protein C in type II pneumocytes. *Am. J. Respir. Cell Mol. Biol.* **26**:659-670.

20. Ueno,T., Linder,S., Na,C.L., Rice,W.R., Johansson,J., and Weaver,T.E. 2004. Processing of pulmonary surfactant protein B by napsin and cathepsin H. *J. Biol. Chem.* **279**:16178-16184.

21. Guttentag,S., Robinson,L., Zhang,P., Brasch,F., Buhling,F., and Beers,M. 2003. Cysteine protease activity is required for surfactant protein B processing and lamellar body genesis. *Am. J. Respir. Cell Mol. Biol.* **28**:69-79.

22. Weaver,M., Yingling,J.M., Dunn,N.R., Bellusci,S., and Hogan,B.L. 1999. Bmp signaling regulates proximal-distal differentiation of endoderm in mouse lung development. *Development* **126**:4005-4015.

23. Angliker,H., Wikstrom,P., Kirschke,H., and Shaw,E. 1989. The inactivation of the cysteinyl exopeptidases cathepsin H and C by affinity-labelling reagents. *Biochem. J.* **262**:63-68.

24. Wu,G.S., Saftig,P., Peters,C., and El-Deiry,W.S. 1998. Potential role for cathepsin D in p53-dependent tumor suppression and chemosensitivity. *Oncogene* **16**:2177-2183.

25. Lu,J., Qian,J., Izvolsky,K.I., and Cardoso,W.V. 2004. Global analysis of genes differentially expressed in branching and non-branching regions of the mouse embryonic lung. *Dev. Biol.* **273**:418-435.

26. Weaver,M., Dunn,N.R., and Hogan,B.L. 2000. Bmp4 and Fgf10 play opposing roles during lung bud morphogenesis. *Development* **127**:2695-2704.

27. Lebeche,D., Malpel,S., and Cardoso,W.V. 1999. Fibroblast growth factor interactions in the developing lung. *Mech. Dev.* **86**:125-136.

28. Barrett,A.J. 1980. Fluorimetric assays for cathepsin B and cathepsin H with methylcoumarylamide substrates. *Biochem. J.* **187**:909-912.

29. Waghray,A., Keppler,D., Sloane,B.F., Schuger,L., and Chen,Y.Q. 2002. Analysis of a truncated form of cathepsin H in human prostate tumor cells. *J. Biol. Chem.* **277**:11533-11538.

30. Austyn,J.M., and Gordon,S. 1981. F4/80, a monoclonal antibody directed specifically against the mouse macrophage. *Eur. J. Immunol.* **11**:805-815.

31. Yayoi,Y., Ohsawa,Y., Koike,M., Zhang,G., Kominami,E., and Uchiyama,Y. 2001. Specific localization of lysosomal aminopeptidases in type II alveolar epithelial cells of the rat lung. *Arch. Histol. Cytol.* **64**:89-97.

32. Flentke,G.R., Baker,M.W., Docterman,K.E., Power,S., Lough,J., and Smith,S.M. 2004. Microarray analysis of retinoid-dependent gene activity during rat embryogenesis:

increased collagen fibril production in a model of retinoid insufficiency. *Dev. Dyn.* **229**:886-898.

33. Desai,T.J., Malpel,S., Flentke,G.R., Smith,S.M., and Cardoso,W.V. 2004. Retinoic acid selectively regulates Fgf10 expression and maintains cell identity in the prospective lung field of the developing foregut. *Dev. Biol.* **273**:402-415.

34. Malpel,S., Mendelsohn,C., and Cardoso,W.V. 2000. Regulation of retinoic acid signaling during lung morphogenesis. *Development* **127**:3057-3067.

35. Zhang,T., Maekawa,Y., Hanba,J., Dainichi,T., Nashed,B.F., Hisaeda,H., Sakai,T., Asao,T., Himeno,K., Good,R.A. et al 2000. Lysosomal cathepsin B plays an important role in antigen processing, while cathepsin D is involved in degradation of the invariant chain inovalbumin-immunized mice. *Immunology* **100**:13-20.

36. Angliker,H., Wikstrom,P., Kirschke,H., and Shaw,E. 1989. The inactivation of the cysteinyl exopeptidases cathepsin H and C by affinity-labelling reagents. *Biochem. J.* **262**:63-68.

37. Wilcox,D., and Mason,R.W. 1992. Inhibition of cysteine proteinases in lysosomes and whole cells. *Biochem. J.* **285 (Pt 2)**:495-502.

38. Kominami,E., Tsukahara,T., Hara,K., and Katunuma,N. 1988. Biosyntheses and processing of lysosomal cysteine proteinases in rat macrophages. *FEBS Lett.* **231**:225-228.

39. Nishimura,Y., and Kato,K. 1988. Identification of latent procathepsin H in microsomal lumen: characterization of proteolytic processing and enzyme activation. *Arch. Biochem. Biophys.* **260**:712-718.

40. Shaw,E. 1994. Peptidyl diazomethanes as inhibitors of cysteine and serine proteinases. *Methods Enzymol.* **244**:649-656.

41. Saftig,P., Hetman,M., Schmahl,W., Weber,K., Heine,L., Mossmann,H., Koster,A., Hess,B., Evers,M., von,F.K. et al 1995. Mice deficient for the lysosomal proteinase cathepsin D exhibit progressive atrophy of the intestinal mucosa and profound destruction of lymphoid cells. *EMBO J.* **14**:3599-3608.

42. Roth,W., Deussing,J., Botchkarev,V.A., Pauly-Evers,M., Saftig,P., Hafner,A., Schmidt,P., Schmahl,W., Scherer,J., nton-Lamprecht,I. et al 2000. Cathepsin L deficiency as molecular defect of furless: hyperproliferation of keratinocytes and pertubation of hair follicle cycling. *FASEB J.* **14**:2075-2086.

43. Bellusci,S., Henderson,R., Winnier,G., Oikawa,T., and Hogan,B.L. 1996. Evidence from normal expression and targeted misexpression that bone morphogenetic protein (Bmp-4) plays a role in mouse embryonic lung morphogenesis. *Development* **122**:1693-1702.

44. Eblaghie,M.C., Reedy,M., Oliver,T., Mishina,Y., and Hogan,B.L. 2006. Evidence that autocrine signaling through Bmpr1a regulates the proliferation, survival and morphogenetic behavior of distal lung epithelial cells. *Dev. Biol.* **291**:67-82.

45. Hyatt,B.A., Shangguan,X., and Shannon,J.M. 2002. BMP4 modulates fibroblast growth factor-mediated induction of proximal and distal lung differentiation in mouse embryonic tracheal epithelium in mesenchyme-free culture. *Dev. Dyn.* **225**:153-165.

46. Vrljicak,P., Myburgh,D., Ryan,A.K., van Rooijen,M.A., Mummery,C.L., and Gupta,I.R. 2004. Smad expression during kidney development. *Am. J. Physiol Renal Physiol* **286**:F625-F633.

47. de Sousa Lopes,S.M., Roelen,B.A., Monteiro,R.M., Emmens,R., Lin,H.Y., Li,E., Lawson,K.A., and Mummery,C.L. 2004. BMP signaling mediated by ALK2 in the visceral endoderm is necessary for the generation of primordial germ cells in the mouse embryo. *Genes Dev.* **18**:1838-1849.

48. Furuta,Y., Piston,D.W., and Hogan,B.L. 1997. Bone morphogenetic proteins (BMPs) as regulators of dorsal forebrain development. *Development* **124**:2203-2212.

49. Constam,D.B., and Robertson,E.J. 2000. SPC4/PACE4 regulates a TGFbeta signaling network during axis formation. *Genes Dev.* **14**:1146-1155.

50. Cui,Y., Hackenmiller,R., Berg,L., Jean,F., Nakayama,T., Thomas,G., and Christian,J.L. 2001. The activity and signaling range of mature BMP-4 is regulated by sequential cleavage at two sites within the prodomain of the precursor. *Genes Dev.* **15**:2797-2802.

51. Cui,Y., Jean,F., Thomas,G., and Christian,J.L. 1998. BMP-4 is proteolytically activated by furin and/or PC6 during vertebrate embryonic development. *EMBO J.* **17**:4735-4743.

52. Aono,A., Hazama,M., Notoya,K., Taketomi,S., Yamasaki,H., Tsukuda,R., Sasaki,S., and Fujisawa,Y. 1995. Potent ectopic bone-inducing activity of bone morphogenetic protein-4/7 heterodimer. *Biochem. Biophys. Res. Commun.* **210**:670-677.

53. Jortikka,L., Laitinen,M., Lindholm,T.S., and Marttinen,A. 1997. Internalization and intracellular processing of bone morphogenetic protein (BMP) in rat skeletal muscle myoblasts (L6). *Cell Signal.* **9**:47-51.

54. Zhu,H., Kavsak,P., Abdollah,S., Wrana,J.L., and Thomsen,G.H. 1999. A SMAD ubiquitin ligase targets the BMP pathway and affects embryonic pattern formation. *Nature* **400**:687-693.

55. Podos,S.D., Hanson,K.K., Wang,Y.C., and Ferguson,E.L. 2001. The DSmurf ubiquitin-protein ligase restricts BMP signaling spatially and temporally during Drosophila embryogenesis. *Dev. Cell* **1**:567-578.

56. Murakami,G., Watabe,T., Takaoka,K., Miyazono,K., and Imamura,T. 2003. Cooperative inhibition of bone morphogenetic protein signaling by Smurf1 and inhibitory Smads. *Mol. Biol. Cell* **14**:2809-2817.

ACKNOWLEDGEMENTS

We thank Mary Jo Murnane, Konstantin Izvolsky, Kim Fisher, Felicia Chen, and Jeff Sedita for helpful discussions. We are also grateful to Xiaoqian Qi, Xiuzhi Tang and Chun Li for technical assistance. This work was supported by the grants NIH/NHLBI PO1 HL47049 and NIH/NHLBI R01 HL67129.

FIGURE LEGENDS

Figure 1. Differential expression of Cathepsin genes in lung epithelial explants undergoing bud morphogenesis in response to FGF10. Mesenchyme-free epithelium from E11.5 lungs were cultured in serum-free medium with human recombinant FGF10, and their transcriptional expression profiles were characterized by Affymetrix oligonucleotide microarray analysis at 0h, 8h, and 24h. Fold changes in Cathepsin gene expression in time (hours) are represented in logarithmic scale in A; table in B depicts fold change with p-value for each of the comparisons.

Figure 2. Expression pattern of Cathepsins in the developing lung and inducibility by FGF10. (A-F), Whole mount in situ hybridization (WMISH) of *Ctsh, Ctsl, Ctsd* and *Ctsz* in E11.5-12 lungs freshly isolated (upper panel), or engrafted with heparin beads soaked in FGF10 and cultured for 48h (bottom panels). In the E12 lung *Ctsh is* highly expressed in the distal epithelium (A), while *Ctsl* is essentially mesenchymal (B) and *Ctsd and Ctsz* are present in both mesenchyme and epithelium (C and D). This pattern is also seen in cultured lungs (A-D, compare arrowheads in upper and bottom panels). *Ctsh* mRNA is dramatically induced in the epithelium adjacent to the FGF10 bead (arrowheads in A and E; compare with negative control PBS bead). E and F depict *Ctsh* antisense (AS) and sense (S) probes, respectively (note only background staining with sense probe). By contrast, FGF10 does not induce expression of the other Cathepsins genes (B-D, lower panel). FGF10 induction of Ctsh is further confirmed by isotopic ISH and immunohistochemistry (arrowheads in G and H). At E11 (I), *Ctsh* expression has not initiated in the lung epithelium (*), but is present in the pulmonary artery (pa, red arrow) near the trachea. At E14 Ctsh is expressed in the distal lung epithelium (J-K, red arrowheads) and scattered mesenchymal cells (K, blue arrowhead). In the adult lung (L) Ctsh is expressed in type II cells (arrowhead), some endothelial cells (red arrow) and macrophages (not shown). Whole mount (A-F, I) and isotopic (G, H) in situ hybridization; immunohistochemistry (H, K, L). Scale bar in (A): 250uM, (F): 300uM and (H):30uM.

Figure 3. Ctsh expression in the developing mouse embryo (immunohistochemistry). (A) Strong Ctsh expression is detected in the visceral endoderm (ve) at E7.0 and at E12 in yolk sac (B-C). Lower levels are detected in the extra embryonic tissue at E7.0 (A). (D-E) Strong Ctsh expression in the E12 choroid plexus and in epithelial tubules of the E14 kidney. Scale bars in (C) and (E): 100uM and 200uM, respectively.

.

Figure 4. Retinoic acid (RA) suppresses FGF10-induced expression of Ctsh in cultured lungs. Control (Ctr), all-trans RA and BMS493-treated E12 lungs engrafted with an FGF10-soaked heparin bead and cultured for 48h. (A) Western blot analysis of Ctsh shows marked decrease in both 28KD and 22KD Ctsh species in RA-treated samples. The RA antagonist BMS493 does not interfere with FGF10-induction of Ctsh because in E12 lungs endogenous RA signaling is already downregulated in distal buds; thus, Ctsh is expressed at comparable levels in controls and BMS-treated lungs. (B-C) Ctsh immunostaining confirms that almost no signals are present in the epithelium surrounding the FGF10 bead of RA-treated lungs(C, asterisks), while strong expression is seen in BMS-treated (B) and control (Fig. 2H) lungs.

Figure 5. Inhibition of Ctsh activity in cultured embryonic lungs and yolk sac membranes. (A) Ctsh activity assay in lungs. The Arg-MCA hydrolyzing activity (pmoles MCA/min/ug protein) was determined in protein extracts from lung cultures initially treated with 1uM or 2uM of Ctshi (*H_2N-Ser(O-Bzl)-CHN_2*) or with DMSO, which were subsequently incubated with Arg-MCA substrate plus DMSO (blue bars) or with Arg-MCA plus Ctshi at 10uM (magenta bars). Bars and lines represent mean plus standard error. Treatment with Ctshi (10uM) significantly reduced the enzymatic activity of the lungs pre-treated with DMSO (Ctr1 and 2, *p <0.05, depicted on the left), but had no further effect in the activity of the lungs pre-treated with Ctshi (1 or 2uM, represented on the left). (B) Western blot analysis of Ctsh in the supernatant and tissue homogenates from E12.5 lungs (top) or E12.5 yolk sacs (bottom) cultured in control or Ctshi-containing media for 48h. Ctshi treatment leads to an increase in abundance and molecular weight of Ctsh protein (both the 28kD and 22kD species) in both the lung and yolk sac samples.

Figure 6. Inhibition of Ctsh activity disrupts lung branching morphogenesis. (A) Ctshi at 1.0 or 2.0uM significantly reduces the number of terminal buds in E12 lungs cultured for 48 hour (26 and 35% reduction relative to control lungs, respectively). Bar and line represent mean ±se (* p< 0.05). (B) PCNA staining of control (DMSO) and Ctshi cultured lungs show abundant expression in distal epithelium of both groups. (C) Treatment of E12 lungs with effective concentrations of Ctsl inhibitor (Ctsli) or Ctsd inhibitor (Ctsdi) have no significant effect on lung branching morphogenesis.

Figure 7. Effect of Ctshi in Fgf10 expression and in Fgf10-mediated responses. (A) Real time quantitative PCR analysis of *Fgf10* mRNA in lungs treated with different cathepsin inhibitors shows a slight increase in levels (~20%, *p<0.05) in the Ctshi group, and no changes in Ctsdi and Ctsli groups (Bar, mean; line, se). (B) Ctshi treatment significantly interferes with the response of the lung epithelium to exogenous FGF10. In control culture medium (B-C) a heparin bead soaked in FGF10, but not PBS, induces a chemoatractant response in the lung epithelium (B, red bracket). Ctshi in the medium inhibits this response (D, blue arrowhead; E).

Figure 8. Inhibition of Ctsh selectively stabilizes mature Bmp4 protein in cultured lungs. (A), non-isotopic ISH shows overlapping expression of *Ctsh* and *Bmp4* in the distal epithelium of cultured lungs. (B-C), Western blot analysis of cultured lungs shows that Ctshi dramatically stabilizes the 18KD mature Bmp4, but not the 51KD Bmp4 precursor protein (compare 18kD a abundance in Ctrl and Ctshi-treated lungs; recombinant mature Bmp4 loaded on the right as reference). This effect is not observed in other Fgf10 targets, such as Spry2 and cannot be reproduced by treatment with Ctsli or Ctsdi. (D) Decreased expression of *Bmp4 mRNA (*Real time PCR, top panel; p<0.05) and increased levels mature Bmp4 (middle panel) in Ctshi-treated lungs. Ctshi treatment also increases mature Bmp4 protein levels in cultured lungs in which new transcription was inhibited by actinomycin D (ActD). Bottom panel represents Western blotting of Ctsh.

A

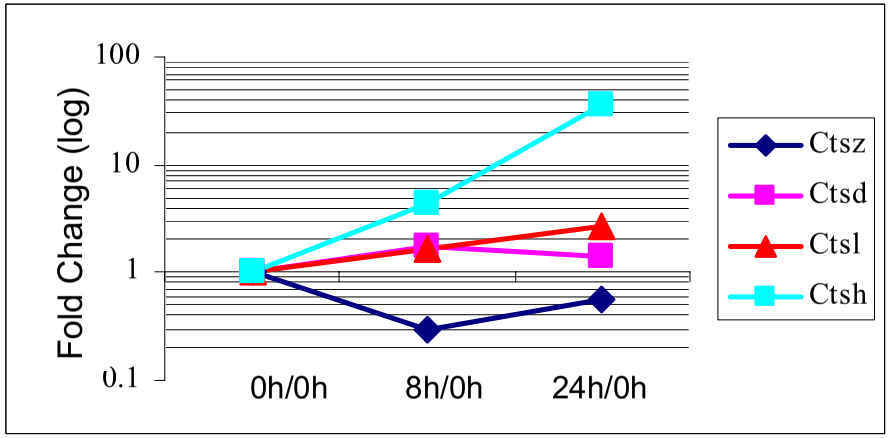

B

fold change (p-value)

	8 h / 0 h	24 h / 0 h
Ctsz	0.3 (0.03)	0.6 (0.05)
Ctsd	1.7 (0.01)	1.4 (0.11)
Ctsl	1.6 (0.45)	2.6 (0.01)
Ctsh	4.5 (0.23)	35.8 (0.01)

Figure 1
Lu et al.

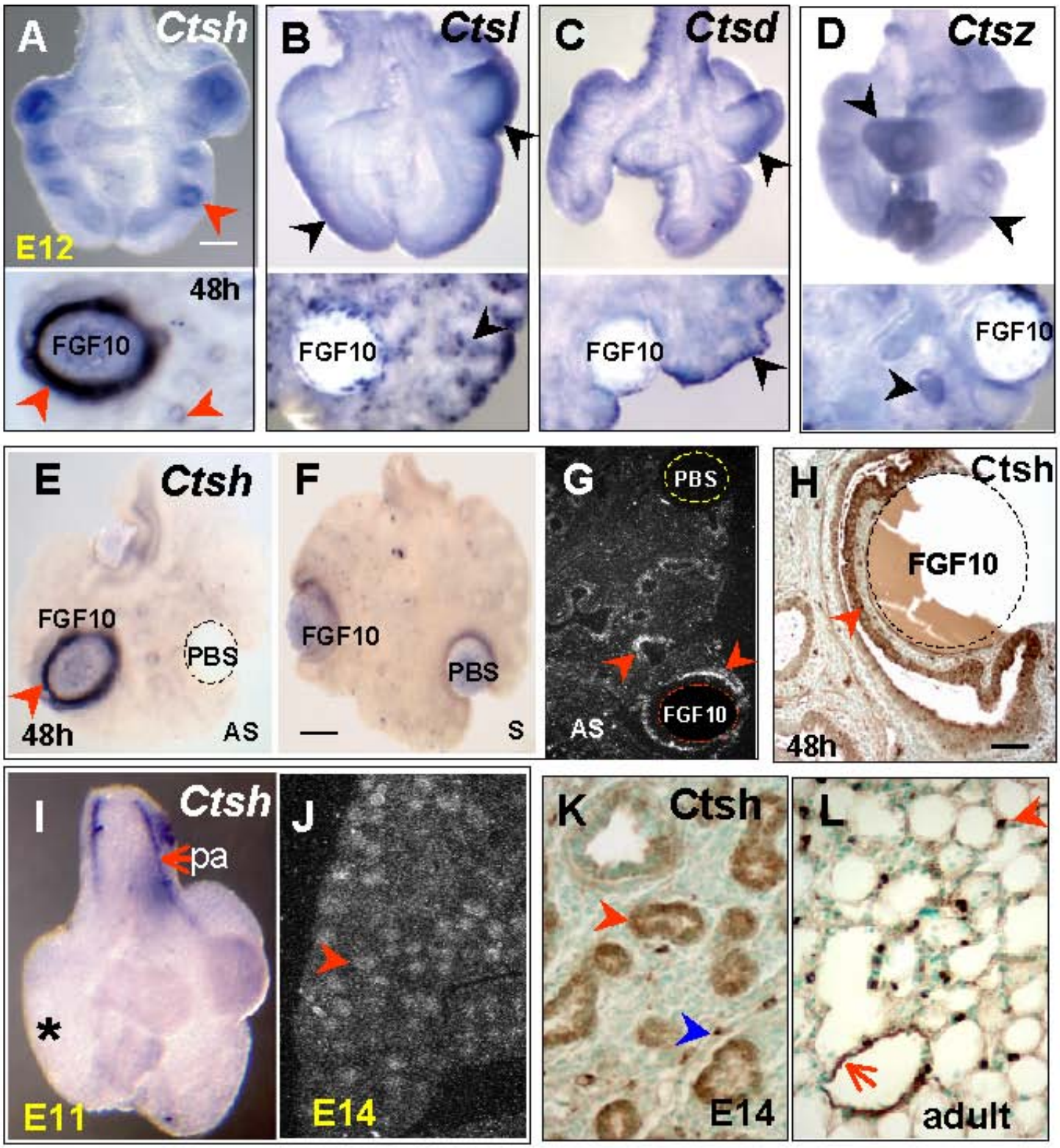

Figure 2
Lu et al.

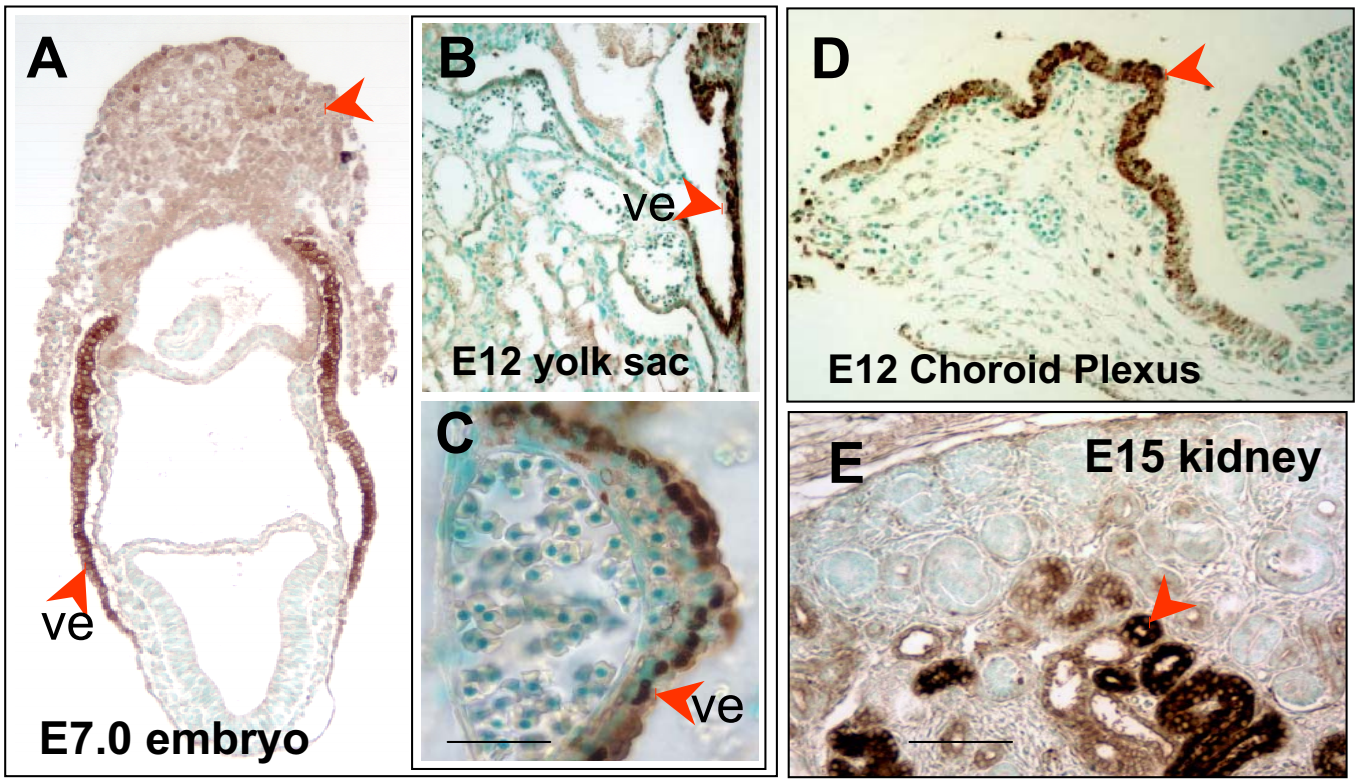

Figure 3
Lu et al.

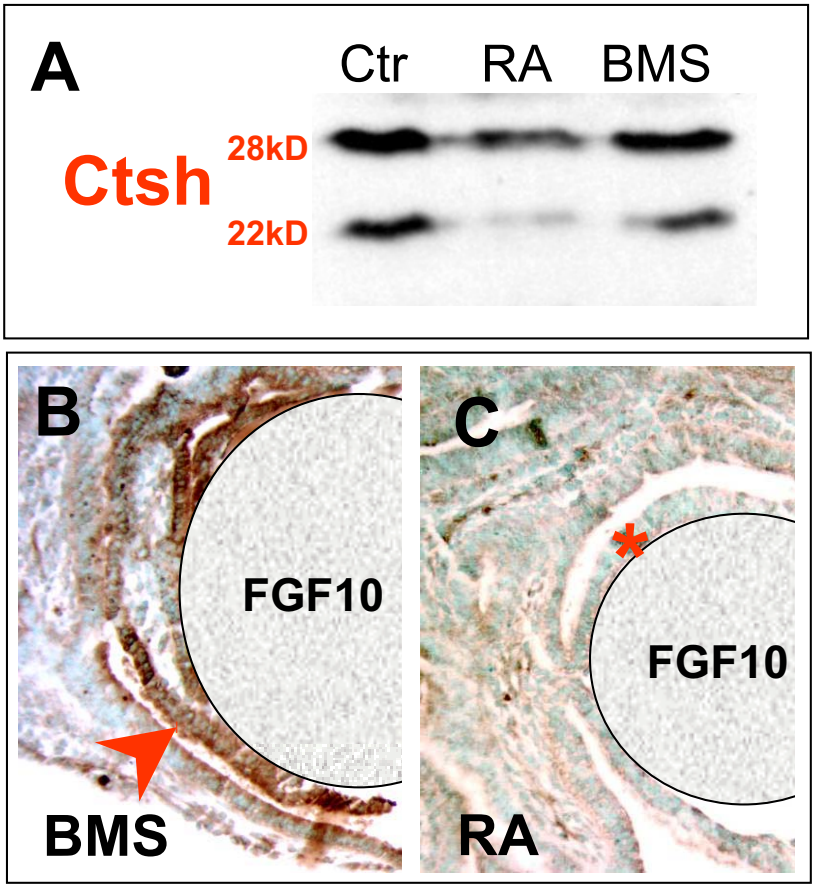

Figure 4
Lu et al.

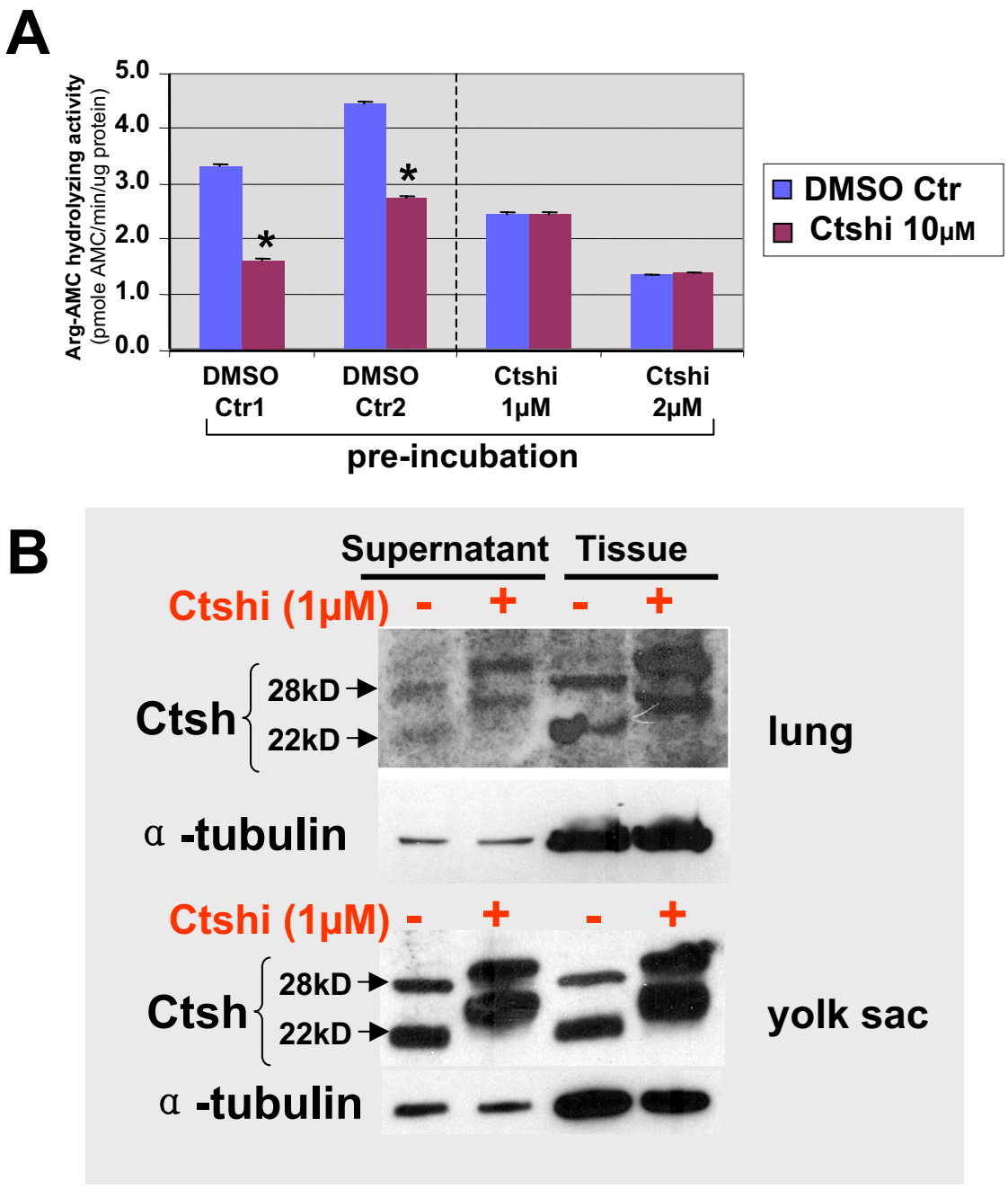

Figure 5
Lu et al.

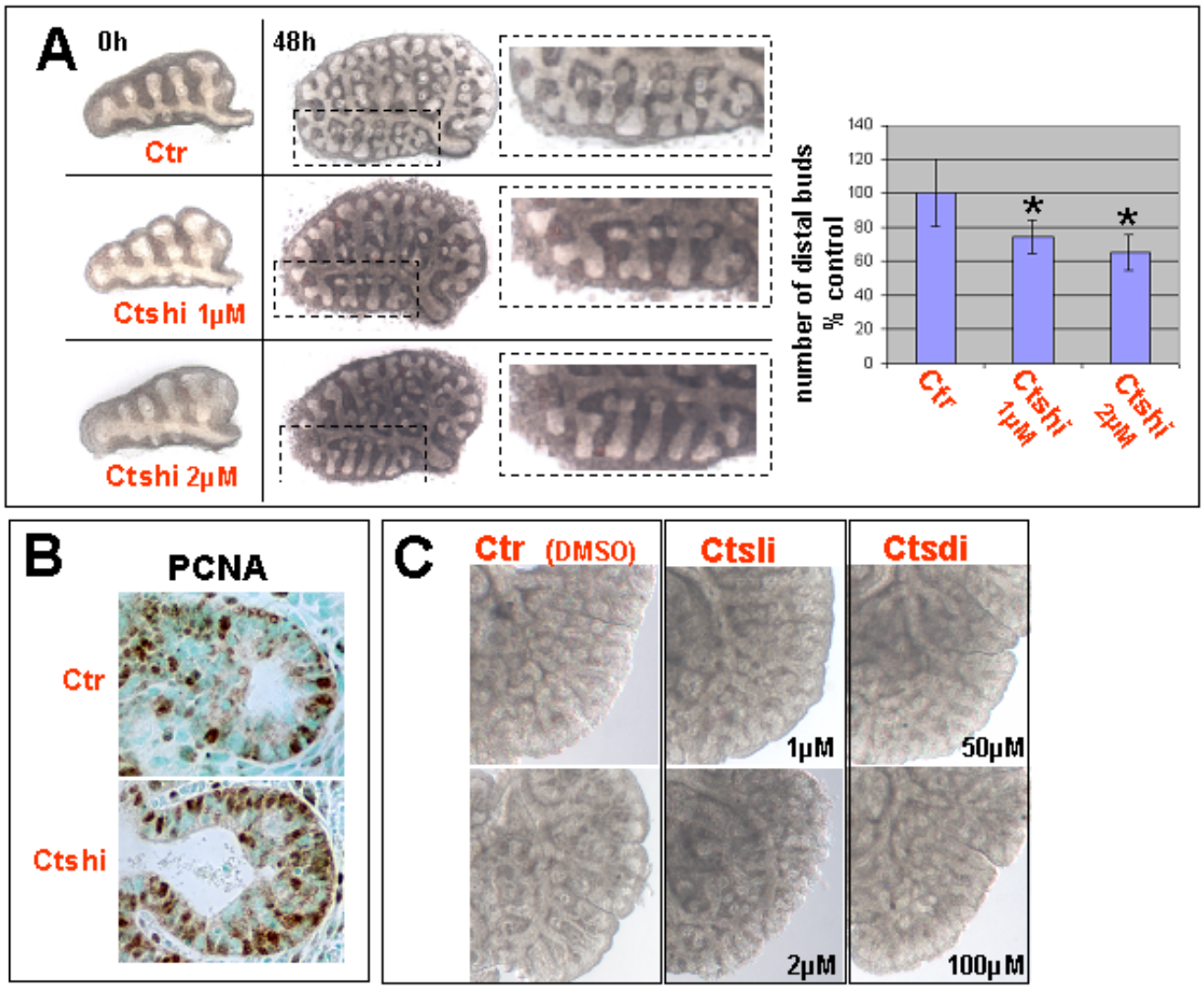

Figure 6
Lu et al.

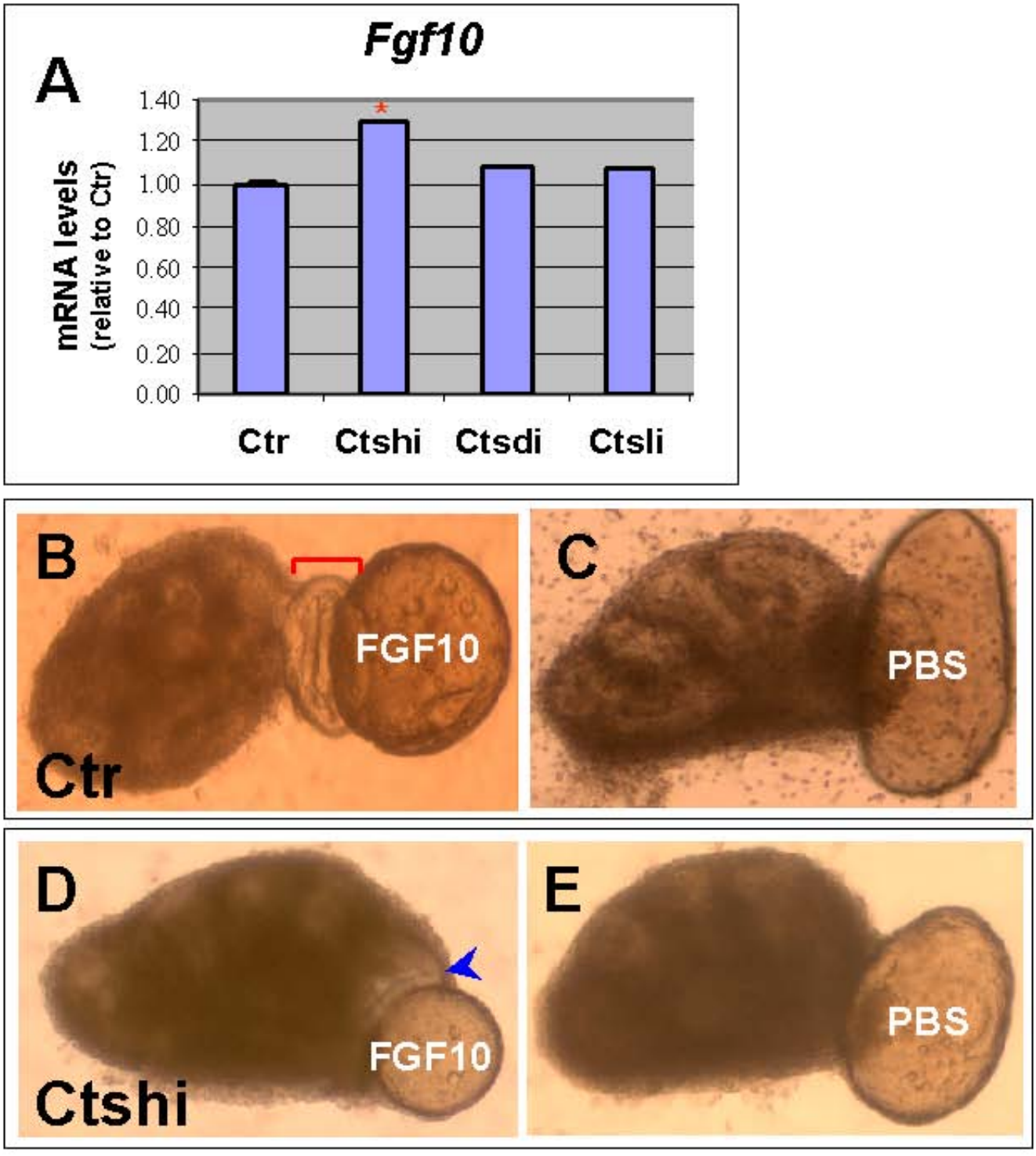

Figure 7
Lu et al.

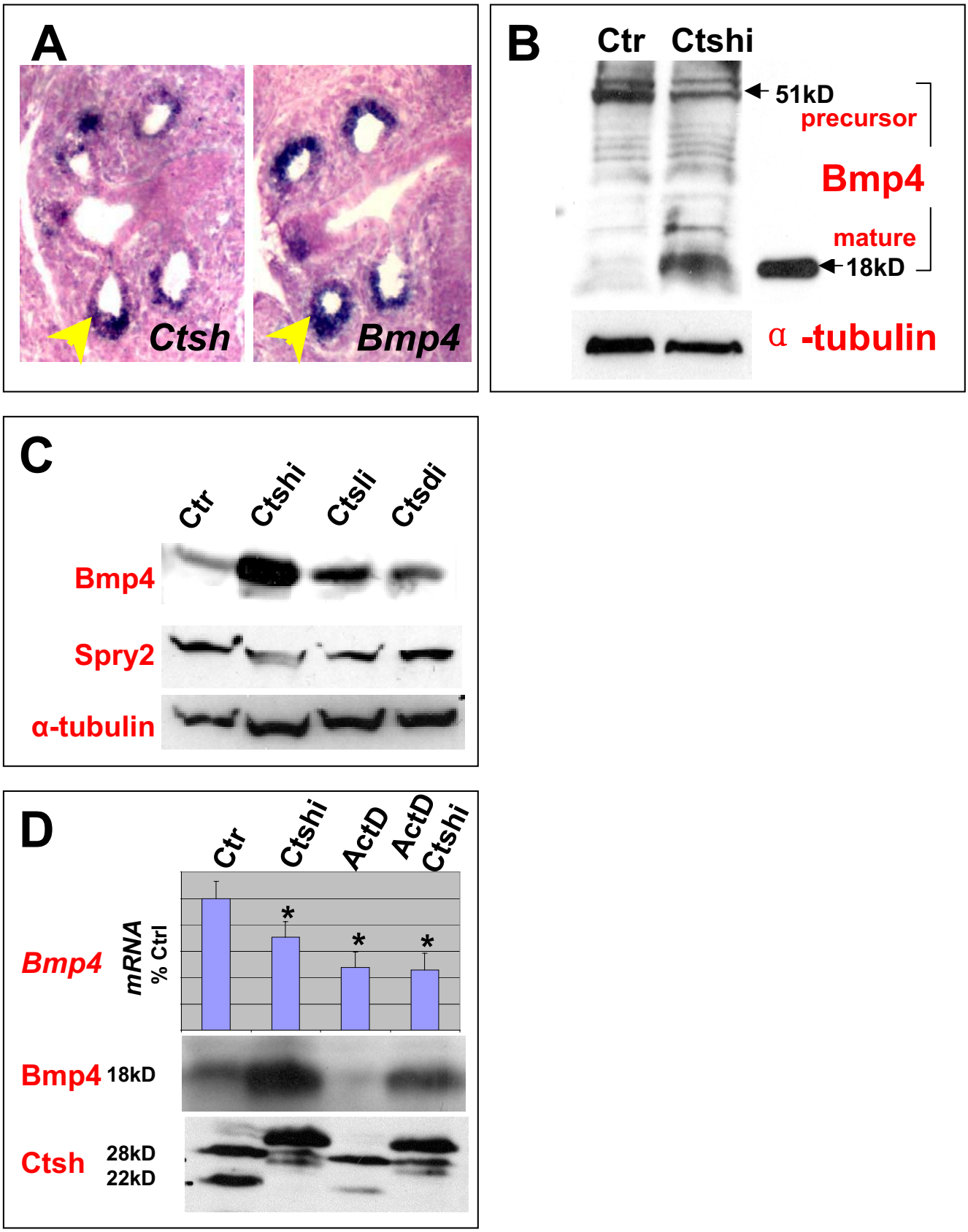

Figure 8
Lu et al.